

Strangeness and Charm in Nuclear Matter

Laura Tolos^{a,b}, Daniel Cabrera^c, Carmen Garcia-Recio^d, Raquel Molina^e, Juan Nieves^f,
Eulogio Oset^f, Angels Ramos^g, Olena Romanets^h, Lorenzo Luis Salcedo^d

^a Instituto de Ciencias del Espacio (IEEC/CSIC), Campus Universitat Autònoma de Barcelona, Facultat de Ciències, Torre C5, E-08193 Bellaterra (Barcelona), Spain

^b Frankfurt Institute for Advanced Studies, Johann Wolfgang Goethe University, Ruth-Moufang-Str. 1, 60438 Frankfurt am Main, Germany

^c Departamento de Física Teórica II, Universidad Complutense, 28040 Madrid, Spain

^d Departamento de Física Atómica, Molecular y Nuclear, and Instituto Carlos I de Física Teórica y Computacional, Universidad de Granada, E-18071 Granada, Spain

^e Research Center for Nuclear Physics (RCNP), Mihogaoka 10-1, Ibaraki 567-0047, Japan

^f Instituto de Física Corpuscular (centro mixto CSIC-UV), Institutos de Investigación de Paterna, Aptdo. 22085, 46071, Valencia, Spain

^g Departament d'Estructura i Constituents de la Matèria, Universitat de Barcelona, Diagonal 647, 08028 Barcelona, Spain

^h Theory Group, KVI, University of Groningen, Zernikelaan 25, 9747 AA Groningen, The Netherlands

Abstract

The properties of strange (K , \bar{K} and \bar{K}^*) and open-charm (D , \bar{D} and D^*) mesons in dense matter are studied using a unitary approach in coupled channels for meson-baryon scattering. In the strangeness sector, the interaction with nucleons always comes through vector-meson exchange, which is evaluated by chiral and hidden gauge Lagrangians. For the interaction of charmed mesons with nucleons we extend the SU(3) Weinberg-Tomozawa Lagrangian to incorporate spin-flavor symmetry and implement a suitable flavor symmetry breaking. The in-medium solution for the scattering amplitude accounts for Pauli blocking effects and meson self-energies. On one hand, we obtain the K , \bar{K} and \bar{K}^* spectral functions in the nuclear medium and study their behaviour at finite density, temperature and momentum. We also make an estimate of the transparency ratio of the $\gamma A \rightarrow K^+ K^{*-} A'$ reaction, which we propose as a tool to detect in-medium modifications of the \bar{K}^* meson. On the other hand, in the charm sector, several resonances with negative parity are generated dynamically by the s -wave interaction between pseudoscalar and vector meson multiplets with $1/2^+$ and $3/2^+$ baryons. The properties of these states in matter are analyzed and their influence on the open-charm meson spectral functions is studied. We finally discuss the possible formation of D -mesic nuclei at FAIR energies.

© 2012 Published by Elsevier Ltd.

Keywords: Strange mesons, transparency ratio, dynamically-generated baryon resonances, open charm in matter, D -mesic nuclei

1. Introduction

Strangeness and charm in hot and dense matter is a matter of extensive analysis in connection to heavy-ion collisions from SIS [1] to FAIR [2] energies at GSI.

In the strange sector, the interaction of strange pseudoscalar mesons (K and \bar{K}) with matter is a topic of high interest. Whereas the interaction of $\bar{K}N$ is repulsive at threshold, the phenomenology of antikaonic atoms [3] shows that the \bar{K} feels an attractive potential at low densities. This attraction is a consequence of the modified s -wave $\Lambda(1405)$ resonance in the medium due to Pauli blocking effects [4] together with the self-consistent consideration of the \bar{K} self-energy [5] and the inclusion of self-energies of the mesons and baryons in the intermediate states [6]. Attraction of the order of -50 MeV at normal nuclear matter density, $\rho_0 = 0.17 \text{ fm}^{-3}$, is obtained in unitarized theories in coupled

channels based on chiral dynamics [6] and meson-exchange models [7, 8]. Moreover, the knowledge of higher-partial waves beyond s -wave [9, 10, 11] becomes essential for relativistic heavy-ion experiments at beam energies below 2A GeV [1]. As for vector mesons in the nuclear medium, only the non-strange ones have been the main focus of attention for years, while very little discussion has been made about the properties of the strange ones, K^* and \bar{K}^* . Only recently the \bar{K}^*N interaction in free space has been addressed in Ref. [12] using SU(6) spin-flavour symmetry, and in Refs. [13, 14] within the hidden local gauge formalism for the interaction of vector mesons with baryons of the octet and the decuplet. Within the scheme of Ref. [13], medium effects have been implemented and analyzed very recently [15] finding an spectacular enhancement of the \bar{K}^* width in the medium.

With regard to the charm sector, the nature of new charmed and strange hadron resonances is an active topic of research, with recent data coming from CLEO, Belle, BaBar and other experiments [16]. In the upcoming years, the experimental program of the future FAIR facility at GSI [2] will also face new challenges where charm plays a dominant role. Approaches based on coupled-channel dynamics have proven to be very successful in describing the experimental data. In particular, unitarized coupled-channel methods have been applied in the meson-baryon sector with charm content [17, 18, 19, 20, 21, 22, 23], partially motivated by the parallelism between the $\Lambda(1405)$ and the $\Lambda_c(2595)$. Other existing coupled-channel approaches are based on the Jülich meson-exchange model [24, 25] or on the hidden gauge formalism [26].

However, these models are not fully consistent with heavy-quark spin symmetry (HQSS) [27], which is a proper QCD symmetry that appears when the quark masses, such as the charm mass, become larger than the typical confinement scale. Aiming at incorporating HQSS, an SU(6) \times SU(2) spin-flavor symmetric model has been recently developed [28, 29], similarly to the SU(6) approach in the light sector of Refs. [12, 30]. The model generates dynamically resonances with negative parity in all the isospin, spin, strange and charm sectors that one can form from an s -wave interaction between pseudoscalar and vector meson multiplets with $1/2^+$ and $3/2^+$ baryons [31]. Recent calculations on bottomed resonances using this HQSS model have also been performed [32].

In this paper we review the properties of the strange (K , \bar{K} and \bar{K}^*) and open-charm (D , \bar{D} and D^*) mesons in dense matter. We address different experimental scenarios that can be analyzed in present and future experiments so as to test the properties of these mesons in matter, such as the transparency ratio of the $\gamma A \rightarrow K^+ K^{*-} A'$ reaction and the formation of D -mesic nuclei.

2. K and \bar{K} mesons in a hot dense nuclear medium

The kaon and antikaon self-energies in symmetric nuclear matter at finite temperature are obtained from the s - and p -waves in-medium kaon-nucleon interaction within a chiral unitary approach [11, 33]. The s -wave amplitude of the $\bar{K}N$ comes, at tree level, from the Weinberg-Tomozawa term of the chiral Lagrangian. Unitarization in coupled channels is imposed on on-shell amplitudes (T) with a cutoff regularization. The $\Lambda(1405)$ resonance in the $I = 0$ channel is generated dynamically and a satisfactory description of low-energy scattering observables is achieved. The KN effective interaction is also obtained from the Bethe-Salpeter equation using the same cutoff parameter.

The in-medium solution of the s -wave amplitude accounts for Pauli-blocking effects, mean-field binding on the nucleons and hyperons via a $\sigma - \omega$ model, and the dressing of the pion and kaon propagators. The self-energy is then obtained in a self-consistent manner summing the transition amplitude T for the different isospins over the nucleon Fermi distribution at a given temperature, $n(\vec{q}, T)$,

$$\Pi_{K(\bar{K})N}(q_0, \vec{q}, T) = \int \frac{d^3p}{(2\pi)^3} n(\vec{p}, T) [T_{K(\bar{K})N}^{(I=0)}(P_0, \vec{P}, T) + 3 T_{K(\bar{K})N}^{(I=1)}(P_0, \vec{P}, T)], \quad (1)$$

where $P_0 = q_0 + E_N(\vec{p}, T)$ and $\vec{P} = \vec{q} + \vec{p}$ are the total energy and momentum of the kaon-nucleon pair in the nuclear matter rest frame, and (q_0, \vec{q}) and (E_N, \vec{p}) stand for the energy and momentum of the kaon and nucleon, respectively, also in this frame. In the case of the \bar{K} meson the model includes, in addition, a p -wave contribution to the self-energy from hyperon-hole (Yh) excitations, where Y stands for Λ , Σ and Σ^* components. For the K meson the p -wave self-energy results from YN^{-1} excitations in crossed kinematics. The self-energy determines, through the Dyson equation, the in-medium kaon propagator and the corresponding kaon spectral function.

The evolution of the \bar{K} and K spectral functions with density and temperature is shown in Fig. 1. The \bar{K} spectral function (left) shows a broad peak that results from a strong mixing between the quasi-particle peak and the

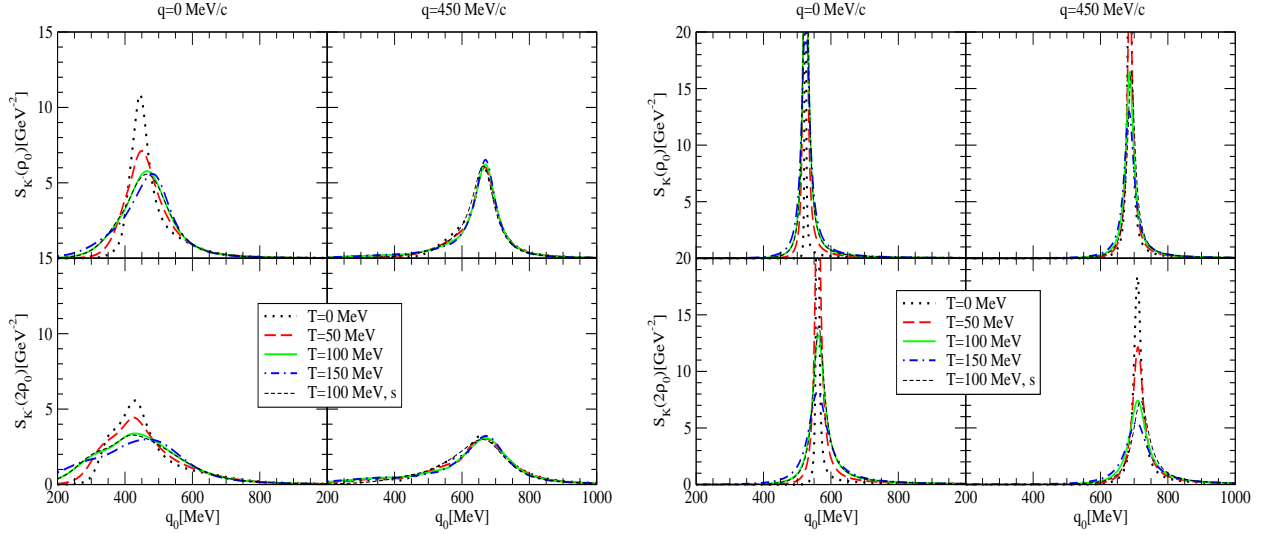


Figure 1. \bar{K} (left) and K (right) spectral functions for different densities, temperatures and momenta.

$\Lambda(1405)N^{-1}$ and $Y(= \Lambda, \Sigma, \Sigma^*)N^{-1}$ excitations. These p -wave YN^{-1} subthreshold excitations affect mainly the properties of the \bar{K} at finite momentum, enhancing the low-energy tail of the spectral function and providing a repulsive contribution to the \bar{K} potential that partly compensates the attraction obtained from the stronger s -wave $\bar{K}N$ interaction component. Temperature and density soften the p -wave contributions to the spectral function at the quasi-particle energy. As for the K meson, the spectral function (right) shows a narrow quasi-particle peak which dilutes with temperature and density as the phase space for KN states increases. With increasing density, the repulsive character of the s -wave KN interaction also increases, thereby shifting the quasi-particle peak of the K spectral function to higher energies.

There has been a lot of activity aiming at extracting the properties of kaons and antikaons in a dense and hot environment from heavy-ion collisions. Some time ago, the antikaon production in nucleus-nucleus collisions at SIS energies was studied using a BUU transport model with antikaons that were dressed with the Juelich meson-exchange model [34]. Multiplicity ratios involving strange mesons coming from heavy-ion collisions data were also analyzed [35]. More recently, a systematic study of the experimental results of KaoS collaboration was performed together with a detailed comparison to transport model calculations [36]. Several conclusions on the production mechanisms for strangeness were achieved. However, to which extent the properties of \bar{K} mesons are modified in matter is not fully understood. There is still no convincing simultaneous description of all experimental data that involve antikaons in matter. These conclusions can also be found in a recent report on strangeness production close to threshold in proton-nucleus and heavy-ion collisions [37].

3. \bar{K}^* meson in matter

The \bar{K}^* self-energy in symmetric nuclear matter is obtained within the hidden gauge formalism [15]. There are two sources for the modification of the \bar{K}^* s -wave self-energy in nuclear matter: a) the contribution associated to the decay mode $\bar{K}^*\pi$ modified by nuclear medium effects on the \bar{K} and π mesons, which accounts for the $\bar{K}^*N \rightarrow \bar{K}N, \pi Y, \bar{K}\pi N, \pi\pi Y \dots$ processes, with $Y = \Lambda, \Sigma$, and b) the contribution associated to the interaction of the \bar{K}^* with the nucleons in the medium, which accounts for the direct quasi-elastic process $\bar{K}^*N \rightarrow \bar{K}^*N$, as well as other absorption channels involving vector mesons, $\bar{K}^*N \rightarrow \rho Y, \omega Y, \phi Y, \dots$. In fact, this last term comes from a unitarized coupled-channel process, similar to the $\bar{K}N$ case. Two resonances are generated dynamically, $\Lambda(1783)$ and $\Sigma(1830)$, which can be identified with the experimentally observed states $J^P = 1/2^-$ $\Lambda(1800)$ and the $J^P = 1/2^-$ PDG state $\Sigma(1750)$, respectively [13].

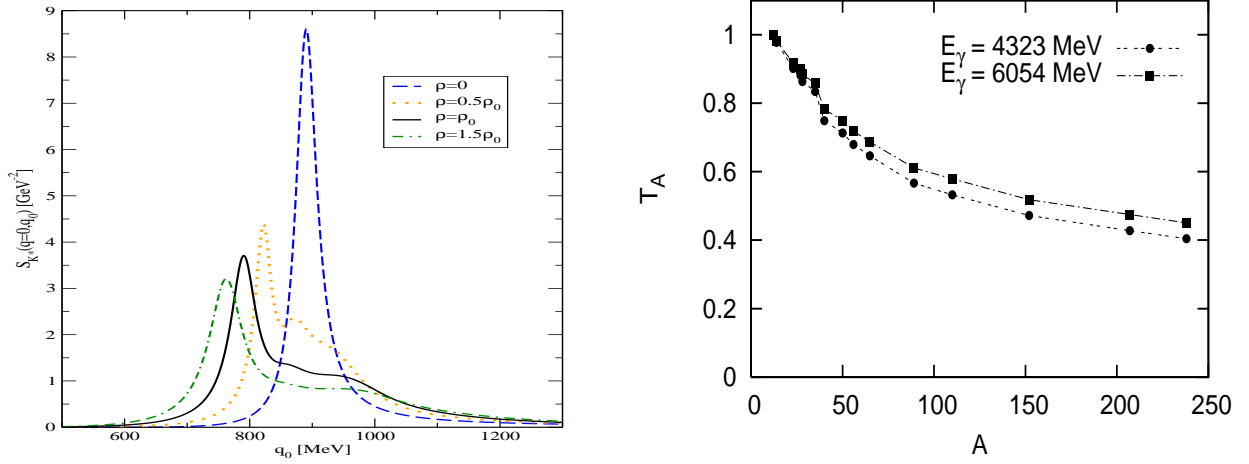


Figure 2. Left: \bar{K}^* spectral function at $\vec{q} = 0$ MeV/c for different densities. Right: Transparency ratio for $\gamma A \rightarrow K^+ K^{*-} A'$

The in-medium \bar{K}^* self-energy results from the sum of both contributions, $\Pi_{\bar{K}^*} = \Pi_{\bar{K}^*}^{(a)} + \Pi_{\bar{K}^*}^{(b)}$, where $\Pi_{\bar{K}^*}^{(b)}$ is obtained, similarly to the \bar{K} meson in Eq. (1), by integrating the \bar{K}^*N transition amplitude over the nucleon Fermi sea.

The \bar{K}^* meson spectral function, which results from the imaginary part of the in-medium \bar{K}^* propagator, is displayed in the left panel of Fig. 2 as a function of the meson energy q_0 , for zero momentum and different densities up to $1.5\rho_0$. The dashed line refers to the calculation in free space, where only the $\bar{K}\pi$ decay channel contributes, while the other three lines correspond to the fully self-consistent calculations, which incorporate the process $\bar{K}^* \rightarrow \bar{K}\pi$ in the medium, as well as the quasielastic $\bar{K}^*N \rightarrow \bar{K}^*N$ and other $\bar{K}^*N \rightarrow VB$ processes. The structures above the quasiparticle peak correspond to the dynamically generated $\Lambda(1783)N^{-1}$ and $\Sigma(1830)N^{-1}$ excitations. Density effects result in a dilution and merging of those resonant-hole states, together with a general broadening of the spectral function due to the increase of collisional and absorption processes. Although the real part of the optical potential is moderate, -50 MeV at ρ_0 , the interferences with the resonant-hole modes push the \bar{K}^* quasiparticle peak to lower energies. However, transitions to meson-baryon states with a pseudoscalar meson, which are included in the \bar{K}^* self-energy but are not incorporated explicitly in the unitarized \bar{K}^*N amplitude, would make the peak less prominent and difficult to disentangle from the other excitations. In any case, what is clear from the present approach, is that the spectral function spread of the \bar{K}^* increases substantially in the medium, becoming at normal nuclear matter density five times bigger than in free space.

3.1. Transparency ratio for $\gamma A \rightarrow K^+ K^{*-} A'$

The nuclear transparency ratio can be studied in order to test experimentally the \bar{K}^* self-energy. The idea is to compare the cross sections of the photoproduction reaction $\gamma A \rightarrow K^+ K^{*-} A'$ in different nuclei, and trace them to the in medium K^{*-} width.

The normalized nuclear transparency ratio is defined as

$$T_A = \frac{\tilde{T}_A}{\tilde{T}_{^{12}\text{C}}} \quad , \text{ with } \tilde{T}_A = \frac{\sigma_{\gamma A \rightarrow K^+ K^{*-} A'}}{A \sigma_{\gamma N \rightarrow K^+ K^{*-} N}} . \quad (2)$$

It describes the loss of flux of K^{*-} mesons in the nucleus and is related to the absorptive part of the K^{*-} -nucleus optical potential and, thus, to the K^{*-} width in the nuclear medium. We evaluate the ratio between the nuclear cross sections in heavy nuclei and a light one (^{12}C), T_A , so that other nuclear effects not related to the absorption of the K^{*-} cancel.

In the right panel of Fig. 2 we show the results for different nuclei. The transparency ratio has been plotted for two different energies in the center of mass reference system $\sqrt{s} = 3$ GeV and 3.5 GeV, which are equivalent to energies

of the photon in the lab frame of 4.3 GeV and 6 GeV, respectively. We observe a very strong attenuation of the \bar{K}^* survival probability due to the decay $\bar{K}^* \rightarrow \bar{K}\pi$ or absorption channels $\bar{K}^*N \rightarrow \bar{K}N, \pi Y, \bar{K}\pi N, \pi\pi Y, \bar{K}^*N, \rho Y, \omega Y, \phi Y, \dots$ with increasing nuclear-mass number A . This is due to the larger path that the \bar{K}^* has to follow before it leaves the nucleus, having then more chances to decay or get absorbed.

4. Open-charm mesons in nuclear matter with heavy-quark spin symmetry

The HQSS predicts that, in QCD, all types of spin interactions involving heavy quarks vanish for infinitely massive quarks. Thus, HQSS connects vector and pseudoscalar mesons containing charmed quarks. Chiral symmetry fixes the lowest order interaction between Goldstone bosons and other hadrons in a model independent way; this is the Weinberg-Tomozawa (WT) interaction. Then, it is very appealing to have a predictive model for four flavors including all basic hadrons (pseudoscalar and vector mesons, and $1/2^+$ and $3/2^+$ baryons) which reduces to the WT interaction in the sector where Goldstone bosons are involved and which incorporates HQSS in the sector where charm quarks participate. Indeed, this is a model assumption which is justified in view of the reasonable semiquantitative outcome of the SU(6) extension in the three-flavor sector [38] and on a formal plausibility on how the SU(4) WT interaction in the charmed pseudoscalar meson-baryon sector comes out in the vector-meson exchange picture.

The model extension is given schematically by

$$\mathcal{L}_{\text{WT}}^{\text{SU}(8)} = \frac{1}{f^2} [[M^\dagger \otimes M]_{63_a} \otimes [B^\dagger \otimes B]_{63}]_1, \quad (3)$$

which represents the interaction between baryons (in the 120 irrep of $\text{SU}(6) \times \text{SU}(2)$) and mesons (in the 63) through t -channel exchange in the 63. In the s -channel, the meson-baryon space reduces into four $\text{SU}(6) \times \text{SU}(2)$ irreps, from which two multiplets **120** and **168** are the most attractive. As a consequence, dynamically-generated baryon resonances are most likely to occur in those sectors, and therefore we will concentrate on states which belong to these two representations. From this Lagrangian, we can extract the potential model for meson-baryon interaction that respects HQSS [31] and solve the on-shell Bethe-Salpeter equation in coupled channels so as to calculate the scattering amplitudes. The poles of the scattering amplitudes are the dynamically-generated baryon resonances.

Dynamically generated states in different charm and strange sectors are predicted within our model [28, 29, 31]. Some of them can be identified with known states from the PDG [39]. This identification is made by comparing the PDG data on these states with the mass, width and, most important, the coupling to the meson-baryon channels of our dynamically-generated poles. In the $C = 1, S = 0, I = 0$ sector, we obtain three Λ_c and one Λ_c^* states. The experimental $\Lambda_c(2595)$ resonance can be identified with the pole that we obtain around 2618.8 MeV as similarly done in Ref. [28]. A second broad Λ_c resonance at 2617 MeV is, moreover, observed with a large coupling to the open channel $\Sigma_c\pi$, very close to the $\Lambda_c(2595)$. This is the same two-pole pattern found in the charmless $I = 0, S = -1$ sector for the $\Lambda(1405)$ [40]. A third spin-1/2 Λ_c resonance is seen around 2828 MeV and cannot be assigned to any experimentally known resonance. With regard to spin-3/2 resonances, we find one located at $(2666.6 - i26.7 \text{ MeV})$ that is assigned to the experimental $\Lambda_c(2625)$. For $C = 1, S = 0, I = 1$ (Σ_c sector), three Σ_c resonances are obtained with masses 2571.5, 2622.7 and 2643.4 MeV and widths 0.8, 188.0 and 87.0 MeV, respectively. Moreover, two spin-3/2 Σ_c resonances are generated dynamically. The first one, a bound state at 2568.4 MeV, is thought to be the charmed counterpart of the $\Sigma(1670)$. The second state at $2692.9 - i33.5 \text{ MeV}$ has not a direct experimental comparison.

The in-medium modifications of these resonant states will have important consequences on the properties of open-charm mesons in matter. These modifications can be studied by analyzing the self-energy of open-charm in the nuclear medium. The self-energy and, hence, spectral function for D and D^* mesons are obtained self-consistently in a simultaneous manner, as it follows from HQSS, by taking, as bare interaction, the extended WT interaction previously described. We incorporate Pauli blocking effects and open charm meson self-energies in the intermediate propagators for the in-medium solution [41]. More specifically, the D and D^* self-energies are obtained by summing the transition amplitude over the Fermi sea of nucleons, as well as over the different spin ($J = 1/2$ for DN , and $J = 1/2, 3/2$ for D^*N) and isospin ($I = 0, 1$) channels.

4.1. D mesic nuclei

D and \bar{D} -meson bound states in ^{208}Pb were predicted in Ref. [42] relying upon an attractive D and \bar{D} -meson potential in the nuclear medium. This potential was obtained within a quark-meson coupling (QMC) model [43]. The

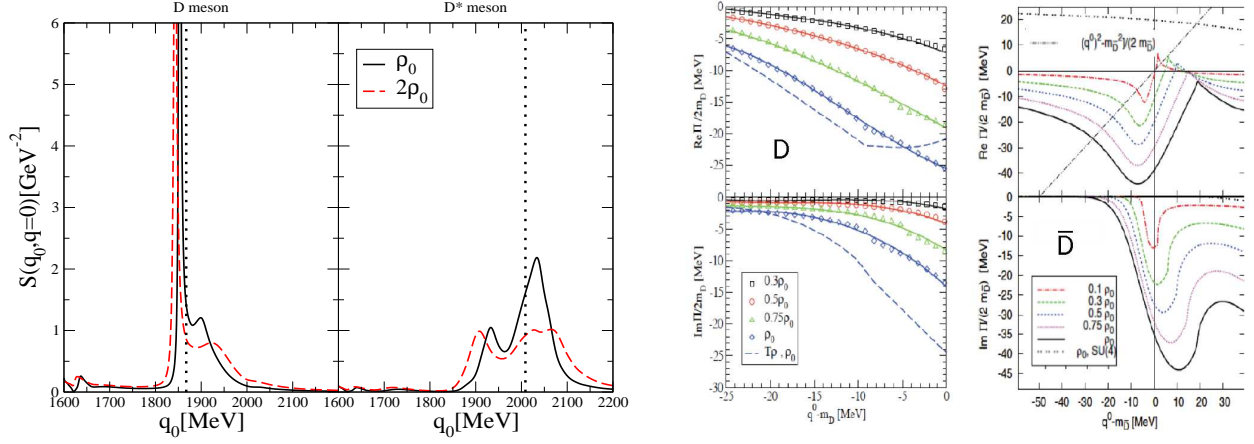


Figure 3. Left: The D and D^* spectral functions in dense nuclear matter at $\vec{q} = 0$ MeV/c. Right: The D and \bar{D} optical potential at $\vec{q} = 0$ MeV/c for different densities

experimental observation of those bound states, though, might be problematic since, even if there are bound states, their widths could be very large compared to the separation of the levels. This is indeed the case for the potential derived from a SU(4) t -vector meson exchange model for D -mesons [22].

We solve the Schrödinger equation in the local density approximation so as to analyze the formation of bound states with charmed mesons in nucleus. We use the energy dependent optical potential

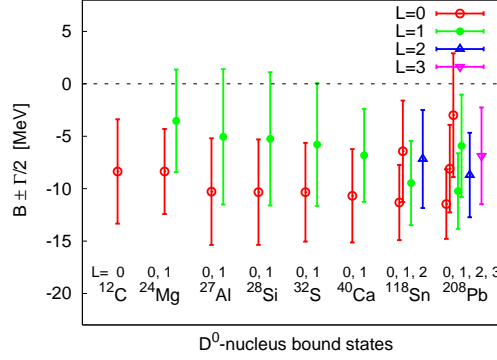
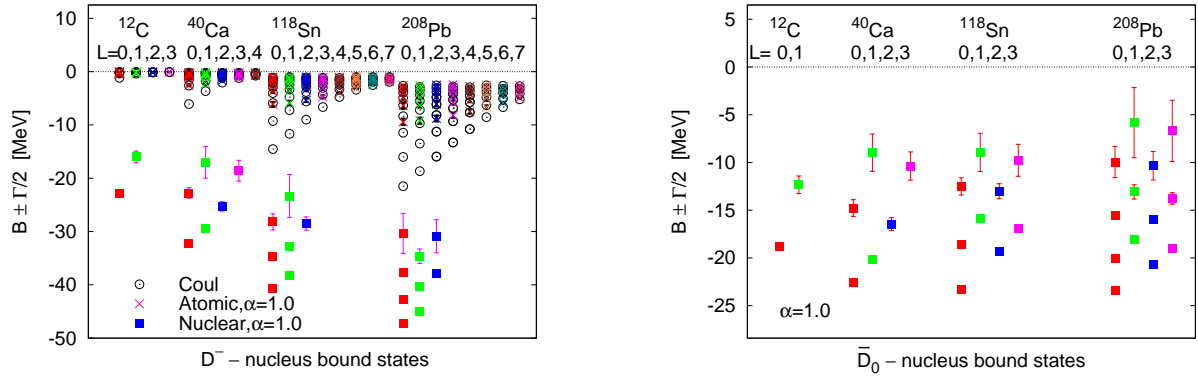
$$V(r, E) = \frac{\Pi(q^0 = m + E, \vec{q} = 0, \rho(r))}{2m}, \quad (4)$$

where $E = q^0 - m$ is the D or \bar{D} energy excluding its mass, and Π the meson self-energy. The optical potential for different densities is displayed on the r.h.s of Fig. 3. For D mesons we observe a strong energy dependence of the potential close to the D meson mass due to the mixing of the quasiparticle peak with the $\Sigma_c(2823)N^{-1}$ and $\Sigma_c(2868)N^{-1}$ states. As for the \bar{D} meson, the presence of a bound state at 2805 MeV [29], almost at $\bar{D}N$ threshold, makes the potential also strongly energy dependent. This is in contrast to the SU(4) model (see Ref. [44]).

The D and D^* spectral functions are displayed on the l.h.s. of Fig. 3. Those spectral functions show a rich spectrum of resonance-hole states. On one hand, the D meson quasiparticle peak mixes strongly with $\Sigma_c(2823)N^{-1}$ and $\Sigma_c(2868)N^{-1}$ states. On the other hand, the $\Lambda_c(2595)N^{-1}$ is clearly visible in the low-energy tail. With regard to the D^* meson, the D^* spectral function incorporates the $J = 3/2$ resonances, and the quasiparticle peak fully mixes with the $\Sigma_c(2902)N^{-1}$ and $\Lambda_c(2941)N^{-1}$ states. For both mesons, the $Y_c N^{-1}$ modes tend to smear out and the spectral functions broaden with increasing phase space, as seen before in the SU(4) model [21]. Note that resonances with higher masses than those described in Sec. 4 are also present in the spectral functions. Those resonant states were seen in the wider energy range explored in Ref. [28] and are not coming from the two most attractive representations, **120** and **168**.

Then, the question is whether D and/or \bar{D} will be bound in nuclei. We observe that the D^0 -nucleus states are weakly bound (see Fig. 4), in contrast to previous results using the QMC model. Moreover, those states have significant widths [44], in particular, for ^{208}Pb [42]. Only D^0 -nucleus bound states are possible since the Coulomb interaction prevents the formation of observable bound states for D^+ mesons.

With regard to \bar{D} -mesic nuclei, not only D^- but also \bar{D}^0 bind in nuclei (Fig. 5). The spectrum contains states of atomic and of nuclear types for all nuclei for D^- while, as expected, only nuclear states are present for \bar{D}^0 in nuclei. Compared to the pure Coulomb levels, the atomic states are less bound. The nuclear ones are more bound and may present a sizable width [45]. Moreover, nuclear states only exist for low angular momenta. It is also interesting to note that a recent work suggests the possibility that, for the lightest nucleus, DNN develops a bound and narrow state with $S = 0, I = 1/2$, as evaluated in Ref. [46].

Figure 4. D^0 -nucleus bound states.Figure 5. D^- and \bar{D}^0 -nucleus bound states.

To gain some knowledge on the charmed meson-nucleus interaction, the information on bound states is very valuable. This is of special interest for PANDA at FAIR. The experimental detection of D and \bar{D} -meson bound states is, however, a difficult task. For example, it was observed in Ref. [44] that reactions with antiprotons on nuclei for obtaining D^0 -nucleus states might have a very low production rate. Reactions but with proton beams seem more likely to trap a D^0 in nuclei [44].

Acknowledgments

This research was supported by DGI and FEDER funds, under Contract Nos. FIS2011-28853-C02-02, FIS2011-24149, FIS2011-24154, FPA2010-16963 and the Spanish Consolider-Ingenio 2010 Programme CPAN (CSD2007-00042), by Junta de Andalucía Grant No. FQM-225, by Generalitat Valenciana under Contract No. PROMETEO/2009/0090, by the Generalitat de Catalunya under contract 2009SGR-1289 and by the EU HadronPhysics3 project, Grant Agreement No. 283286. O. R. wishes to acknowledge support from the Rosalind Franklin Programme. L. T. acknowledges support from Ramon y Cajal Research Programme, and from FP7- PEOPLE-2011-CIG under Contract No. PCIG09-GA- 2011-291679.

References

- [1] C. Fuchs, Prog. Part. Nucl. Phys. 56 (2006) 1.

- [2] <http://www.gsi.de/fair>
- [3] E. Friedman and A. Gal, Phys. Rept. 452 (2007) 89.
- [4] V. Koch, Phys. Lett. B 337 (1994) 7.
- [5] M. Lutz, Phys. Lett. B 426 (1998) 12.
- [6] A. Ramos and E. Oset, Nucl. Phys. A 671 (2000) 481.
- [7] L. Tolos, A. Ramos, A. Polls and T. T. S. Kuo, Nucl. Phys. A 690 (2001) 547.
- [8] L. Tolos, A. Ramos and A. Polls, Phys. Rev. C 65 (2002) 054907.
- [9] L. Tolos, A. Ramos and E. Oset, Phys. Rev. C 74 (2006) 015203.
- [10] M. F. M. Lutz, C. L. Korpa and M. Moller, Nucl. Phys. A 808 (2008) 124.
- [11] L. Tolos, D. Cabrera and A. Ramos, Phys. Rev. C 78 (2008) 045205.
- [12] C. Garcia-Recio, J. Nieves, and L. L. Salcedo, Phys. Rev. D 74 (2006) 034025.
- [13] E. Oset and A. Ramos, Eur. Phys. J. A 44 (2010) 445.
- [14] K. P. Khemchandani, H. Kaneko, H. Nagahiro and A. Hosaka, Phys. Rev. D 83 (2011) 114041; K. P. Khemchandani, A. Martinez Torres, H. Kaneko, H. Nagahiro and A. Hosaka, Phys. Rev. D 84 (2011) 094018; K. P. Khemchandani, A. Martinez Torres, H. Nagahiro and A. Hosaka, Phys. Rev. D 85 (2012) 114020
- [15] L. Tolos, R. Molina, E. Oset and A. Ramos, Phys. Rev. C 82 (2010) 045210
- [16] <http://www.lepp.cornell.edu/Research/EPP/CLEO/>; <http://belle.kek.jp/>; <http://www.slac.stanford.edu/BF/>
- [17] L. Tolos, J. Schaffner-Bielich and A. Mishra, Phys. Rev. C 70 (2004) 025203.
- [18] L. Tolos, J. Schaffner-Bielich and H. Stoecker, Phys. Lett. B 635 (2006) 85
- [19] M. F. M. Lutz and E. E. Kolomeitsev, Nucl. Phys. A 730 (2004) 110.
- [20] J. Hofmann and M. F. M. Lutz, Nucl. Phys. A 763 (2005) 90; J. Hofmann and M. F. M. Lutz, Nucl. Phys. A 776 (2006) 17.
- [21] T. Mizutani and A. Ramos, Phys. Rev. C 74 (2006) 065201.
- [22] L. Tolos, A. Ramos and T. Mizutani, Phys. Rev. C 77 (2008) 015207
- [23] C. E. Jimenez-Tejero, A. Ramos and I. Vidana, Phys. Rev. C 80 (2009) 055206.
- [24] J. Haidenbauer, G. Krein, U. G. Meissner and A. Sibirtsev, Eur. Phys. J. A 33 (2007) 107 .
- [25] J. Haidenbauer, G. Krein, U. G. Meissner and L. Tolos, Eur. Phys. J A 47 (2011) 18.
- [26] J. -J. Wu, R. Molina, E. Oset and B. S. Zou, Phys. Rev. Lett. 105 (2010) 232001.
- [27] N. Isgur, M. B. Wise, Phys. Lett. B 232 (1989) 113 ; M. Neubert, Phys. Rept. 245 (1994) 259; A. V. Manohar and M. B. Wise, Camb. Monogr. Part. Phys. Nucl. Phys. Cosmol. 10 (2000) 1.
- [28] C. Garcia-Recio, V. K. Magas, T. Mizutani, J. Nieves, A. Ramos, L. L. Salcedo and L. Tolos, Phys. Rev. D 79 (2009) 054004.
- [29] D. Gamermann, C. Garcia-Recio, J. Nieves, L. L. Salcedo and L. Tolos, Phys. Rev. D 81 (2010) 094016 .
- [30] H. Toki, C. Garcia-Recio and J. Nieves, Phys. Rev. D 77 (2008) 034001.
- [31] O. Romanets, L. Tolos, C. Garcia-Recio, J. Nieves, L. L. Salcedo and R. G. E. Timmermans, Phys. Rev. D 85 (2012) 114032.
- [32] C. Garcia-Recio, J. Nieves, O. Romanets, L. L. Salcedo and L. Tolos, arXiv:1210.4755 [hep-ph].
- [33] D. Cabrera, A. Polls, A. Ramos and L. Tolos, Phys. Rev. C 80 (2009) 045201.
- [34] W. Cassing, L. Tolos, E. L. Bratkovskaya and A. Ramos, Nucl. Phys. A 727 (2003) 59
- [35] L. Tolos, A. Polls, A. Ramos and J. Schaffner-Bielich, hot and dense matter,” Phys. Rev. C 68 (2003) 024903
- [36] A. Forster, F. Uhlig, I. Bottcher, D. Brill, M. Debowski, F. Dohrmann, E. Grosse and P. Koczon *et al.*, Phys. Rev. C 75 (2007) 024906
- [37] C. Hartnack, H. Oeschler, Y. Leifels, E. L. Bratkovskaya and J. Aichelin, Phys. Rept. 510 (2012) 119
- [38] D. Gamermann, C. Garcia-Recio, J. Nieves and L. L. Salcedo, Phys. Rev. D 84 (2011) 056017.
- [39] K. Nakamura *et al.* [Particle Data Group Collaboration], J. Phys. G 37 (2010) 075021.
- [40] D. Jido, J. A. Oller, E. Oset, A. Ramos and U. G. Meissner, Nucl. Phys. A 725 (2003) 181.
- [41] L. Tolos, C. Garcia-Recio, and J. Nieves, Phys. Rev. C 80 (2009) 065202.
- [42] K. Tsushima, D. H. Lu, A. W. Thomas, K. Saito, and R. H. Landau, Phys. Rev. C 59 (1999) 2824.
- [43] P. A. M. Guichon, Phys. Lett. B 200 (1988) 235.
- [44] C. Garcia-Recio, J. Nieves and L. Tolos, Phys. Lett. B 690 (2010) 369.
- [45] C. Garcia-Recio, J. Nieves, L. L. Salcedo and L. Tolos, Phys. Rev. C 85 (2012) 025203.
- [46] M. Bayar, C. W. Xiao, T. Hyodo, A. Dote, M. Oka and E. Oset, Phys. Rev. C 86 (2012) 044004